

Nonmonotonic evolution of out-of-plane resistivity with Pr doping in $Y_{1-x}Pr_xBa_2Cu_3O_{7-\delta}$ single crystals

C. N. Jiang, A. R. Baldwin, G. A. Levin, T. Stein, and C. C. Almasan
Department of Physics, Kent State University, Kent, Ohio 44242

D. A. Gajewski, S. H. Han, and M. B. Maple
Department of Physics and Institute for Pure and Applied Physical Sciences, University of California,
San Diego, La Jolla, California 92093
(Received 3 October 1996)

In-plane (ρ_{ab}) and out-of-plane (ρ_c) resistivities of $Y_{1-x}Pr_xBa_2Cu_3O_{7-\delta}$ have been determined using the electrical contact configuration of the dc flux transformer. $\rho_c(x)$ varies nonmonotonically with x : $\rho_c(x)$ increases at low x , reaches a maximum at $x \approx 0.42$, and then decreases for higher values of x . In contrast, $\rho_{ab}(x)$ increases monotonically with x . These results, along with the coexistence of metallic ρ_{ab} and semiconducting ρ_c , are consistent with the presence of a gap in the energy spectrum of the CuO chains, leading to tunneling through both valence and conduction bands of the CuO chains. [S0163-1829(97)52306-X]

Some of the more interesting and striking aspects of the normal-state resistivity of the high-temperature superconductors are the coexistence of metallic in-plane resistivity $\rho_{ab}(T)$ and semiconducting out-of-plane resistivity $\rho_c(T)$ at low temperatures in a certain range of doping, and the transformation of both resistivities from metallic to insulating in the strongly underdoped regime.¹ This behavior is observed in several underdoped cuprates and is typified by oxygen deficient $YBa_2Cu_3O_y$,^{1,2} where ρ_{ab} , ρ_c , and the anisotropy ρ_c/ρ_{ab} increase *monotonically* with decreasing y . In $YBa_2Cu_3O_y$, the removal of oxygen from the CuO chains has a twofold effect on ρ_c : one is the reduction of the number of holes on the CuO₂ planes through hole filling and their subsequent localization, the other is the drastic change of the condition for tunneling between the neighboring bilayers due to the introduction of oxygen vacancies on the chains. Consequently, one is unable to separate the effect on ρ_c of hole filling and localization on the planes from that of the depletion of the chain layers. It is important to clarify the relationship between the c -axis transport and the transformation of the CuO₂ planes from metallic to insulating (a process intimately related to superconductivity) since one of the fundamental questions about the c -axis transport is its implications for superconductivity of the layered cuprates.

We address this issue through resistivity measurements of fully oxygenated $Y_{1-x}Pr_xBa_2Cu_3O_{7-\delta}$ in which T_c can be continuously "tuned" from 92 to 0 K by increasing the Pr concentration. The Y-Pr sheets, which serve as "internal" charge reservoirs, are located inside the CuO₂ bilayers and, as shown by optical reflectivity measurements,³ do not affect the structure and composition of the blocking layers, which include the CuO chains. Therefore, the c -axis resistivity of $Y_{1-x}Pr_xBa_2Cu_3O_{7-\delta}$ changes only as a result of the transformations that take place in the conduction mechanism of the CuO₂ planes, while the structure of the CuO chains remains unaffected.

Our principal finding is that the evolution of ρ_c is profoundly different in this system than in $YBa_2Cu_3O_y$. In

$Y_{1-x}Pr_xBa_2Cu_3O_y$, $\rho_c(x)$ and the anisotropy $\rho_c(x)/\rho_{ab}(x)$ are *nonmonotonic* functions of x : at low to moderate x , $\rho_c(x)$ and $\rho_c(x)/\rho_{ab}(x)$ increase, reaching a maximum at $x \approx 0.42$; for even higher x values, $\rho_c(x)$ and $\rho_c(x)/\rho_{ab}(x)$ decrease, while $\rho_{ab}(x)$ continues to increase monotonically. In the samples with low Pr concentration both resistivities are metallic; more heavily doped samples exhibit metallic $\rho_{ab}(T)$ and semiconducting $\rho_c(T)$, while both resistivities of the strongly underdoped crystals (very low T_c or nonsuperconducting) are semiconducting at low temperatures. As discussed subsequently, the nonmonotonic evolution of $\rho_c(x)$ and the coexistence of metallic $\rho_{ab}(T)$ and semiconducting $\rho_c(T)$ are consistent with the c -axis charge transport produced by tunneling between a neighboring bilayer and chain-layer, provided there is a gap in the energy spectrum of the CuO chains, so that, in heavily doped $Y_{1-x}Pr_xBa_2Cu_3O_{7-\delta}$, tunneling takes place in the tails of the Fermi distribution.

Single crystals of $Y_{1-x}Pr_xBa_2Cu_3O_{7-\delta}$ with $0.13 \leq x \leq 0.55$ and $0 \leq T_c \leq 85$ K were grown by a method described elsewhere.⁴ Typical sizes of the crystals are $1.0 \times 0.8 \times 0.04$ mm³, with the c -axis oriented along the smallest dimension. Eight electrodes were fabricated on each sample by bonding 1 mil Au wires to the crystal with Ag paste. The typical contact resistance of a completed electrode is 1.8 Ω or less. The distance between the voltage leads is about 1/3 of the length of the crystal.

We determined the resistivities $\rho_c(T, x)$ and $\rho_{ab}(T, x)$ using the electrical contact configuration of the dc flux transformer [inset to Fig. 1(a) shows the configuration of the leads]. A 0.1 mA current biases the top face of the crystal and the voltages on the top (V_{top}) and bottom (V_{bot}) faces are recorded as a function of temperature.⁵⁻⁷ The two-dimensional distribution of the electrical potential $V(x, z)$ inside the crystal is determined by Laplace's equation $\text{div} \vec{j}(x, z) = \rho_{ab}^{-1} \partial^2 V / \partial x^2 + \rho_c^{-1} \partial^2 V / \partial z^2 = 0$, where $\vec{j}(x, z)$ is the current density.⁷ A general solution is given by an infinite series with the coefficients determined from the boundary

conditions. For the voltage drop on the bottom face of the crystal, we obtained the following *rapidly* converging series:

$$V_{\text{bot}} = \frac{8I(\rho_c \rho_{ab})^{1/2}}{\pi b} \sum_{k=0}^{\infty} \frac{(-1)^k}{2k+1} \frac{\sin[(2k+1)\pi d/2L]}{\sinh[(2k+1)\xi\pi D/L]}, \quad (1)$$

where $\xi = (\rho_c/\rho_{ab})^{1/2}$, I is the applied current, b , L , and D are the width, length, and thickness of the sample, respectively, and d is the distance between the two voltage contacts.

In contrast, the voltage distribution on the top face is given by a very *slowly* converging series. The same type of problem appears in the Montgomery method.^{8,9} We solved it by separating the series into slowly and rapidly converging parts. The former is chosen in such a way that it does not depend on ρ_c/ρ_{ab} and can be calculated exactly [the first term on the right-hand side of Eq. (2)], while the rapidly converging series can be easily evaluated numerically. Then,

$$V_{\text{top}} = \frac{8I(\rho_c \rho_{ab})^{1/2}}{\pi b} \left[\frac{1}{2} \ln \tan \left(\frac{\pi}{4} + \frac{\pi d}{4L} \right) + \sum_{k=0}^{\infty} \frac{(-1)^k}{2k+1} \sin \frac{(2k+1)\pi d}{2L} \times \left(\coth \frac{(2k+1)\xi\pi D}{L} - 1 \right) \right] \quad (2)$$

For our $Y_{1-x}\text{Pr}_x\text{Ba}_2\text{Cu}_3\text{O}_{7-\delta}$ samples, the parameter $\xi\pi D/L \geq 1$ ($V_{\text{top}}/V_{\text{bot}} \geq 1$). Even for these relatively small values of anisotropy, it was sufficient to retain only the first three terms ($k=0,1,2$) in Eqs. (1) and (2) to obtain convergence within 0.1%.¹⁰

Special care was taken to ensure that our results reflect bulk properties and are not affected by extrinsic factors such as sample inhomogeneities or surface quality. Two sets of measurements were performed for each sample in which the current was injected through leads 1,4 and 5,8, respectively. The corresponding sets of V_{top} , V_{bot} were compared, and, after correcting for small differences in the spacing between the contacts, only those crystals for which both the corresponding sets of V_{top} , V_{bot} were within 10% of each other were retained for the analysis.

In-plane and out-of-plane resistivities of five $Y_{1-x}\text{Pr}_x\text{Ba}_2\text{Cu}_3\text{O}_{7-\delta}$ single crystals are shown in Fig. 1. The magnitude and temperature dependences of ρ_{ab} [Fig. 1(a)] are very similar to those obtained by a four-point method on a different set of $Y_{1-x}\text{Pr}_x\text{Ba}_2\text{Cu}_3\text{O}_{7-\delta}$ single crystals with current leads mounted on their edges.¹¹ This fact corroborates the correctness of our algorithm. Figure 1(a) shows that $\rho_{ab}(T, x)$ is metallic for $x \leq 0.42$ [i.e., $\rho_{ab}(T) \propto T^{-1} \sim T + \text{const}$] and increases monotonically with increasing Pr content. The sample with $x=0.42$ exhibits early signs of weak localization which indicates that the mobility threshold E_c is close to the Fermi energy of this sample. The samples with $x > 0.42$ display a semiconducting-type behavior of $\rho_{ab}(T)$ at low T . As in all underdoped cuprates, there is a characteristic change of slope $d\rho_{ab}/dT$ at temperatures $T^*(x)$ marked by arrows.¹² This feature is discussed in Ref. 13.

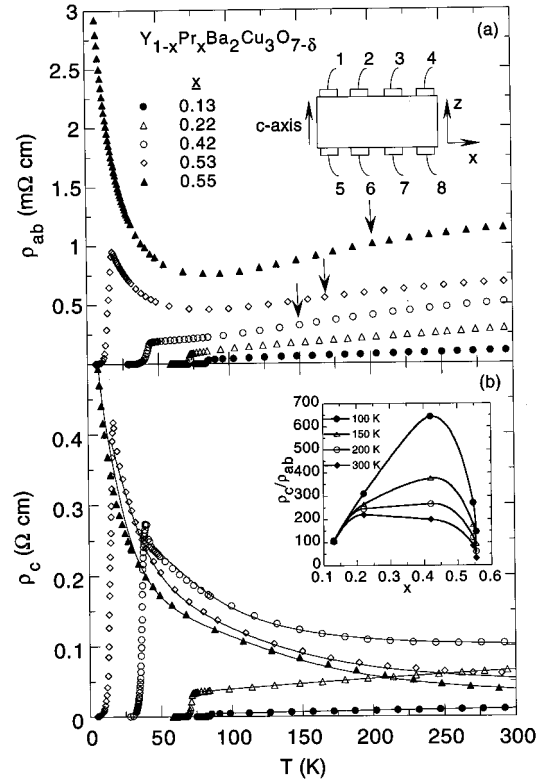


FIG. 1. (a) In-plane resistivity $\rho_{ab}(T)$ and (b) out-of-plane resistivity $\rho_c(T)$ for $Y_{1-x}\text{Pr}_x\text{Ba}_2\text{Cu}_3\text{O}_{7-\delta}$ single crystals. The solid lines in (b) are fits to the data with Eq. (3). Inset to Fig. 1(a): The leads configuration used in our measurements. Inset to Fig. 1(b): Anisotropy ρ_c/ρ_{ab} vs Pr concentration x at different temperatures. The solid lines are guides to the eye.

As shown in Fig. 1(b), the evolution of $\rho_c(x, T)$ is quite surprising. With increasing Pr concentration, $Y_{1-x}\text{Pr}_x\text{Ba}_2\text{Cu}_3\text{O}_{7-\delta}$ exhibits a nonmonotonic variation of $\rho_c(x)$: for low values of x , it increases, reaching a maximum for $x \approx 0.42$, while for even higher Pr concentration, $\rho_c(x, T)$ decreases even though it remains semiconducting. This effect can be illustrated even more dramatically by plotting the anisotropy ρ_c/ρ_{ab} as a function of x at a given temperature [inset to Fig. 1(b)]. Notice that the anisotropy is strongly temperature-dependent in the sample with the highest anisotropy ($x=0.42$), in contrast to optimally doped $\text{YBa}_2\text{Cu}_3\text{O}_{7-\delta}$ (Ref. 14) and strongly underdoped $Y_{1-x}\text{Pr}_x\text{Ba}_2\text{Cu}_3\text{O}_{7-\delta}$ ($x=0.53$ and 0.55) samples.

Figures 1(a) and 1(b) also show that both $\rho_{ab}(T)$ and $\rho_c(T)$ of the $x=0.13$ and 0.22 samples are metallic down to T_c . The $x=0.42$ sample exhibits a coexistence of metallic $\rho_{ab}(T)$ and semiconducting $\rho_c(T)$ at all $T > T_c$. The strongly underdoped samples ($x=0.53$ and 0.55) exhibit a minimum in $\rho_{ab}(T)$ and semiconducting $\rho_c(T)$. Hence, the major features of the resistivity of $Y_{1-x}\text{Pr}_x\text{Ba}_2\text{Cu}_3\text{O}_{7-\delta}$ are the nonmonotonic evolution of $\rho_c(T)$ with Pr content, the transformation of both resistivities from metallic to semiconducting, and the coexistence of metallic $\rho_{ab}(T)$ and semiconducting $\rho_c(T)$ for a certain range of doping.

In a short paper it is difficult to give due credit to many ingenious models of the c -axis transport that have been proposed (see Ref. 1). None, however, have anticipated the nonmonotonic evolution of $\rho_c(x)$ in the underdoped regime. We

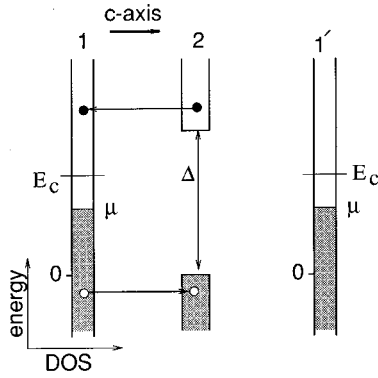


FIG. 2. (a) Schematic representation of the density of states DOS of neighboring bilayers (1) and (1') and the chain layer (2). The latter has a gap Δ between the valence and conduction bands. The shown location of μ results in a semiconducting $\rho_c(T)$ and metallic $\rho_{ab}(T)$. The arrows indicate the two channels of elastic tunneling in the tails of the Fermi distribution.

present here a simple model which attempts to incorporate the main features we described above. Figure 2 illustrates the basic idea of our model. The main contribution to the c -axis conductivity is assumed to be due to the incoherent elastic tunneling between the neighboring CuO_2 bilayer and the CuO chain layer. Then, the transformation of $\rho_c(T)$ from metallic to semiconducting and its nonmonotonic evolution can be understood if we assume that there is a gap Δ in the energy spectrum of the chains. The magnitude and temperature dependence of $\rho_c(T)$ is determined by the location of the chemical potential with respect to the valence and conduction bands of the chains as follows: when the chemical potential lies below the gap, in the valence band, the chains are metallic and so is $\rho_c(T)$; when the Fermi energy enters the gap, tunneling takes place only in the tails of the Fermi distribution through both valence and conduction bands of the chains leading to a semiconducting-type temperature dependence of $\rho_c(T)$ characterized by two activation energies, μ and $\Delta - \mu$ (the maximum value of ρ_c and the strongest temperature dependence corresponding to μ lying in the midgap region); when μ is raised above midgap level, the c -axis conductivity increases due to enhanced current through the conduction band, and at low temperatures $\rho_c(T)$ is governed by the smaller of the two activation energies $\Delta - \mu$. We see that the monotonic change in the position of the chemical potential leads to a nonmonotonic variation of ρ_c .

To test the applicability of this phenomenological model to the $\text{Y}_{1-x}\text{Pr}_x\text{Ba}_2\text{Cu}_3\text{O}_{7-\delta}$ system, we fit our experimental data of all five samples¹⁵ with the following equation for conductivity:^{16,17}

$$\sigma_c = \frac{a\tau_{ab}}{e^{\beta\mu} + 1} + \frac{b}{e^{\beta(\Delta-\mu)} + 1} \equiv \sigma_1 + \sigma_2, \quad (3)$$

where a and b are constants, $\beta = 1/k_B T$, σ_1 and σ_2 are the contributions to σ_c from tunneling through the valence and conduction bands, respectively, and μ is measured from the top of the valence band; we take the relaxation rate $\tau_{ab}^{-1} \propto \tau_s^{-1} + T$, where $\tau_s^{-1} = \text{const}$ is the elastic scattering rate.

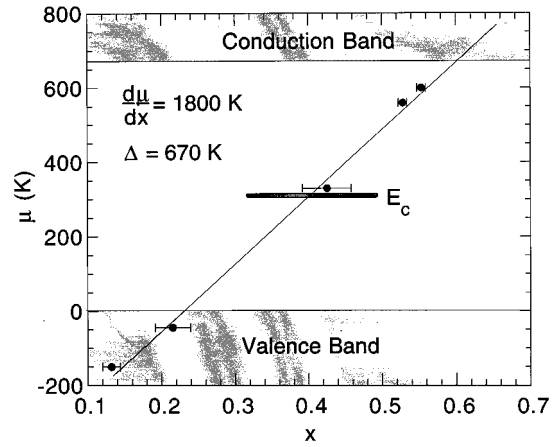


FIG. 3. Chemical potential μ vs Pr concentration x . The solid line is a linear fit. Also shown are a schematic representation of the valence and conduction bands of the chains and the approximate position of the mobility edge E_c .

The fits to $\rho_c(T)$ are shown in Fig. 1(b), while the values of $\mu(x)$ and Δ obtained from the fitting are shown in Fig. 3. The energy gap $\Delta = 670$ K was kept constant during the fitting procedure for all five samples. As shown in Fig. 3, for $x = 0.13$ and 0.22 , the chemical potential is in the valence band ($\mu < 0$) and, therefore, according to Eq. (3), $\rho_c(T)$ is metallic, i.e., $\rho_c(T) \propto \rho_{ab}(T) \propto \tau_{ab}^{-1}$. When $\mu(x)$ enters the gap ($0 < \mu < E_c$), $\rho_c(T)$ becomes semiconducting with two activation energies, μ and $\Delta - \mu$, while $\rho_{ab}(T)$ remains metallic. Finally, when μ is elevated above E_c , both $\rho_{ab}(T)$ and $\rho_c(T)$ become semiconducting at low temperatures, but with different activation energies: $\mu - E_c$ and $\Delta - \mu$, respectively.

The solid line in Fig. 3 is a linear fit to $\mu(x)$ data which gives a slope $d\mu/dx = 1800$ K. An analysis of the in-plane resistivity of the $\text{Y}_{1-x}\text{Pr}_x\text{Ba}_2\text{Cu}_3\text{O}_{7-\delta}$ crystals from an entirely different prospective yields a very close value of $d\mu/dx \approx 1760$ K.¹³ According to Fig. 3, for $x > 0.6$, the chemical potential enters the conduction band making chains “metallic” again, at least in the sense that there is a finite density of states at the Fermi level. This conclusion is corroborated by the evidence of “metallic” chains and insulating planes in aligned films of $\text{PrBa}_2\text{Cu}_3\text{O}_{7-\delta}$.¹⁸

Our model indicates a monotonic increase of the chemical potential with Pr content at an approximately constant rate. This can be easily understood in terms of a hole depletion and subsequent localization process due to a valence of Pr greater than 3. In spite of many experiments, there is no consensus on the nature of the suppression of superconductivity by Pr doping in the $\text{Y}_{1-x}\text{Pr}_x\text{Ba}_2\text{Cu}_3\text{O}_{7-\delta}$ mainly because the chemical valence of Pr remains uncertain. While susceptibility, Hall effect, and neutron-diffraction crystallographic studies indicate that Pr valence is greater than 3, high-energy spectroscopy and band structure calculations indicate an oxidation state Pr^{3+} .¹⁹ Recent optical reflectivity results³ and calculations by Fehrenbacher and Rice²⁰ support the hole depletion mechanism. Reference 20 shows that the total probability of the $4f^1\text{Pr}$ configuration is roughly 0.15–0.2 which may explain the spectroscopic results revealing a

valence $\approx \text{Pr}^{3+}$. The effect of Pr on T_c suppression and conduction in $\text{Bi}_2\text{Sr}_2(\text{Ca}_{1-x}\text{Pr}_x)\text{Cu}_2\text{O}_{8+\delta}$, where hole filling by Pr clearly takes place, is similar to that in $\text{Y}_{1-x}\text{Pr}_x\text{Ba}_2\text{Cu}_3\text{O}_{7-\delta}$.²¹ This also points toward the hole filling and subsequent localization scenario.

The notion that tunneling in the c direction takes place in the tails of the Fermi distribution is similar to that proposed by Abrikosov.¹⁶ However, unlike Ref. 16, we believe that in the fully oxygenated $R\text{Ba}_2\text{Cu}_3\text{O}_{7-\delta}$ (R =rare earth) compounds, this is due to the gap in the density of states (DOS) of the chain layers and not the presence of resonant tunneling

centers. In other cuprates that do not possess metallic chains in the blocking layers and are much more anisotropic, the resonant centers may play a role in the c -direction transport.

We thank A. A. Abrikosov and B. W. Veal for making available to us their work on c -axis resistivity prior to publication, and K. F. Quader for useful discussions. The work at KSU was supported by the Research Council of Kent State University and the National Science Foundation under Grant No. DMR-9601839, and at USCD by the U.S. Department of Energy under Grant No. DE-FG03-86ER-45230.

-
- ¹S. L. Cooper and K. E. Gray, in *Physical Properties of High Temperature Superconductors IV*, edited by D. M. Ginsberg (World Scientific, Singapore, 1994), p. 61.
- ²K. Takenaka, K. Mizuhashi, H. Takagi, and S. Uchida, *Phys. Rev. B* **50**, 6534 (1994); B. W. Veal (unpublished).
- ³K. Takenaka, Y. Imanaka, K. Tamasaku, T. Ito, and S. Uchida, *Phys. Rev. B* **46**, 5833 (1992).
- ⁴L. M. Paulius, B. W. Lee, M. B. Maple, and P. K. Tsai, *Physica C* **230**, 255 (1994).
- ⁵I. Giaever, *Phys. Rev. Lett.* **15**, 825 (1965).
- ⁶H. Safar, E. Rodriguez, F. de la Cruz, P. L. Gammel, L. F. Schneemeyer, and D. J. Bishop, *Phys. Rev. B* **46**, 14 238 (1992).
- ⁷R. Busch, G. Ries, H. Werthner, G. Kreiselmeyer, and G. Saemann-Ischcenko, *Phys. Rev. Lett.* **69**, 522 (1992).
- ⁸H. C. Montgomery, *J. Appl. Phys.* **42**, 2971(1971).
- ⁹B. F. Logan, S. O. Rice, and R. F. Wick, *J. Appl. Phys.* **42**, 2975 (1971).
- ¹⁰In Ref. 7, the expressions for V_{top} and V_{bot} were derived by truncating the slowly converging series, keeping only the $k=0$ term. Therefore, their expressions of V_{top} and V_{bot} do not coincide with Eqs. (1) and (2) even in the limit of large anisotropy $\xi\pi D/L \gg 1$. Moreover, we find that for systems with low or moderate anisotropy, such as $\text{Y}_{1-x}\text{Pr}_x\text{Ba}_2\text{Cu}_3\text{O}_{7-\delta}$, the method of Ref. 7 seriously underestimates ρ_c and distorts its temperature dependence.
- ¹¹M. B. Maple, C. C. Almasan, C. L. Seaman, S. H. Han, K. Yoshikawa, M. Buchgeister, L. M. Paulius, B. W. Lee, D. A. Gajewski, R. F. Jarnim, C. R. Fincher, Jr., Graciela B. Blanchet, and R. P. Guertin, *J. Supercond.* **7**, 97 (1994).
- ¹²B. Batlogg *et al.*, *Physica C* **235-240**, 130 (1994), and references therein.
- ¹³G. A. Levin and K. F. Quader (unpublished).
- ¹⁴T. A. Friedmann, M. W. Rabin, J. Giapintzakis, J. P. Rice, and D. M. Ginsberg, *Phys. Rev. B* **42**, 6217 (1990).
- ¹⁵The $\sigma_c(T)$ of the nonsuperconducting sample ($x=0.55$) was fitted with Eq. (3) for $T \geq 10$ K; below 10 K, both $\rho_c(T)$ and $\rho_{ab}(T)$ exhibit variable range hopping.
- ¹⁶A. A. Abrikosov, *Phys. Rev. B* **52**, 7026 (1995); *Physica C* **258**, 53 (1996).
- ¹⁷N. Kumar and A. M. Jayannavar, *Phys. Rev. B* **45**, 5001 (1992).
- ¹⁸M. Lee, Y. Suzuki, and T. H. Geballe, *Phys. Rev. B* **51**, 15 619 (1995).
- ¹⁹For a review, see, e.g., H. B. Radousky, *J. Mater. Res.* **7**, 1917 (1992).
- ²⁰R. Fehrenbacher and T. M. Rice, *Phys. Rev. Lett.* **70**, 3471 (1993), and references therein.
- ²¹B. Beschoten, S. Sadewasser, G. Guntherodt, and C. Quitmann, *Phys. Rev. Lett.* **77**, 1837 (1996).